

Article

Feasibility Study of Sensor Aided Impact Acoustic Sorting of Plastic Materials from End-of-Life Vehicles (ELVs)

Jiu Huang ^{†,*}, Zhengfu Bian [†] and Shaogang Lei [†]

School of Environmental Science and Spatial Informatics, China University of Mining and Technology, Daxue Rd. 1, Xuzhou 221116, China; E-Mails: zfbian@cumt.edu.cn (Z.B.); lsgang@126.com (S.L.)

[†] These authors contributed equally to this work.

* Author to whom correspondence should be addressed; E-Mail: jhuang@cumt.edu.cn; Tel.: +86-516-8388-3100; Fax: +86-516-8359-1330.

Academic Editor: Samuel B. Adeloju

Received: 16 September 2015 / Accepted: 2 December 2015 / Published: 9 December 2015

Abstract: The purpose of this feasibility research was to study a novel sensor based separation method for recycling of plastic materials from end-of-life vehicles (ELVs) by using eigen-frequency response of impact acoustic emission. In this research three kinds of commonly used plastics, polypropylene (PP), acrylonitrile-butadiene-styrene (ABS), and styrene-maleic-anhydride (SMA) sampled from end-of-life vehicles, were researched. Almost all the crushed plastic scraps had a flake structure, theoretically their impact response behaviors were determined by their diameters and thicknesses. The equivalent diameters of the scraps were characterized by fine sieving and their thicknesses were measured online by a 3D laser triangulation sensor above the conveying path. Following this the scraps were free dropped one-by-one to impact with an impact passive body on which impact acoustic emission (AE) signals were generated and acquired by an acoustic pickup sensor. Thirdly, the AE signals which carried eigen-frequency response features were processed and characterized. Results demonstrated that the scraps with diameters < 8 mm were too weak for the actual devices to process; the scraps with diameter from 8–13 mm still generated quite a lot of AE signals of inadequate intensity. Finally the general characterization and recognition yields were 64.6%, 61.7%, and 63.9% of PP, ABS, and SMA in mass, respectively of tested materials.

Keywords: end-of-life vehicles (ELVs) recycling; automobile shredder residues (ASRs); sensor aided sorting; impact acoustic emission (AE)

1. Introduction

With the rapid increase of retaining of worldwide vehicles, and considering the conservation of raw material resources as well as environmental impacts, the disposal and cyclic utilization of end-of-life vehicles (ELVs) have achieved much attention over the last decade. The Economic Cooperation and Development organization (OECD) has projected that the growth of vehicles could achieve 32% from 1997 to 2020 [1–4]. China has occupied the first position of global automobile production and sale since 2009, and worldwide in this year more than 13.6 million vehicles were produced and sold; meanwhile 2.7 million ELVs were abandoned. Vehicle retaining in China is estimated as up to 150 million vehicles until 2020. At this time, the domestic yield by of ELVs could achieve 9 million annually in China, with an abandon rate of 6%. Disposal and recovery of ELVs has become an important scientific, economic and social issue in China [5,6]. Without clean disposal and recovery methods, ELVs could be a hazard to environment and ecological systems [7,8]. However, in China the relevant industry is only just beginning.

EU countries have made significant progress on disposal and recovery of ELVs. About 75% (mass basis) of ELVs are recycled and reused, but there still remains 25% in mass, named as automobile shredder residues (ASRs) or car fluffs. ASR is a solid waste mixture with extremely high heterogeneity. ASR contains moisture, ferrous and nonferrous metals, plastics, rubber, mineral materials like glass, dust, foam materials, fibers, woody materials, textiles *etc.* Due to the high heterogeneity and complex composition ASRs are classified as Hazardous Material and the EU generates about 2–3 Mt ASRs annually [1–4,7–9].

Due to high polymer content, ASR has an average lower heat value of about 20 MJ/kg [10], therefore thermal recovery processes are widely used for their energetic recovery, such as incineration, pyrolysis, and gasification. Thermal processes convert organic materials of ASR into energy or fuels but concentrate chlorine, heavy metals, and toxins present in ASR, in the ash residues [10–12], which leads to environmental risks. Moreover, the increasingly strict regulations concerning gaseous emissions also limits the thermal processes [12]. Hence according to relevant EU Directives (2000/532/EC, 2001/18/EC2, 2001/119/EC3, and 2001/573/EC4) on ELVs, after January 2015, the disposal and recovery of ELVs should achieve a recoverability rate of 95% (mass), among which the recyclability and reuse rate should achieve 85%. In China there are similar directives (National Development and Reform Commission Proclamation 2006/9) which govern the ELV recoverability rate and should achieve 95% by 2017, among which recyclability/reuse should achieve 85%. ASR Landfill will be progressively prohibited. However, ASR occupies normally 20%–25% of original ELV mass, and it is believed it will keep increasing due to the usage of plastic materials in vehicles instead of metals. Therefore in order to reduce the yield of ASR and to achieve the requirements of directives, novel post shredder technologies (PST) for advanced materially recycling of plastic materials from ELVs for feedstock material are required both in the EU and China [13–17].

Commonly plastics take up about 40% of ASR mass, these are a more valuable part but mixed with other materials in ASR, especially engineering plastics. Fine recycling of ELV plastic fractions to produce secondary plastic materials can be an appropriate method to satisfy the relevant directives. There are conventional PST recycling processes such as the VW-SiCon process, GALLOO process, Argonne's 4th flotation process *etc.* for recycling of ELV plastic fractions. However, they are only able to selectively separate restricted kinds of plastic mixture products—only specific kinds of plastic like PVC get sorted individually. The mixture products normally contain two to three kinds of plastics with purities around 50%–60% [18,19]. These PST recycling technologies could provide plastic mixture products from ELVs but fail in the sorting of plastic materials individually and then producing pure plastic products. Further, more precise sorting technologies like sensor aided sorting methods could be applied.

In addition to traditional PST for recycling of ELV plastics, in the last decade, novel sorting methods of indirect material detection, such as recognition by using different sensor technologies and then a material separation process by using additional force field (like a compressed air nozzle) have been developed and implemented in processing and recycling processes. These kinds of sorting technologies are called “Sensor Based Sorting” or “Sensor Aided Sorting”, and are defined as single grain separation for contact-free detection of externally identifiable and measurable separation parameters. This technology has brought revolution to the design of dry separation processes in solid industrial waste recycling and mineral processing. These techniques allow the design of material recovery processes with high sorting efficiency, which lead to enhanced resource efficiency and therefore to a higher grade of sustainability [20]. Professional sensor aided sorting technologies for waste plastic recycling have also been developed and applied, such as visual optical sorting, near infrared (NIR) and middle infrared (MIR) sorting, tribo-electrification sorting *etc.* However, all of them are incapable of sorting ASR plastics. Since visual optical sorters are only available for color detection, they cannot distinguish different materials with homochromatic features; an NIR spectral detector is able to distinguish most kinds of plastics with high precision but it is not available for black and dark dyed polymers, such as plastics used in vehicles and electronic products, since black and dark dye like soot absorbs nearly 100% of NIR radiation and results in inadequate reflection. The MIR spectral method generates sufficient reflected signals on the surface of black and dark dyed polymers but this method takes several minutes for material recognition, which hampers its industrial utilization; vehicle plastics are always modified and reinforced by padding with different additives like talc. Additives have an influence on the tribo-electrification properties of plastics, hence the tribo-electrification sorter for commonly used plastics is no longer applicable to ASR plastic recycling [21–26].

Also, over the last decade, sensor aided sorting by using impact Acoustic Emission (AE) has been developed and applied for fine processing and refinery. This technology was first applied in the food industry, for example it has been utilized for nuts such as pistachio or walnut separation [23]. During their growth period some nut pieces are empty or infested by insects with some pupals or mature insects inside. These damaged pieces of nuts need to be eliminated from intact ones. However, to investigate the inner part of nuts is difficult and some internal investigation method like radioactive measurement is not appropriate for foods. Hence the technology of using impact AE was developed. Impact acoustic sorting is a non-destructive method which does not need to break physical or chemical structures of the tested objects. The precondition is that impact must occur in the range of elastic collision on both bodies. During the impact process, part of the kinetic energy of the active impact rigid body is

transferred to both impact bodies in the form of vibrations. Then the vibration of the impact bodies is further transferred into ambient air, which results in acoustic wave emission (AE), *i.e.*, the sounds propagate in all directions. The impact AE and impact bodies have the same vibrational frequency response which is caused by the impact process, therefore an impact acoustic emission carries information of the corresponding impact. Properties of impact AE signal are associated with the characteristics of the impact body and its material. Compared with optical sensors, impact AE has much less data to be processed which leads to a very high speed both of recognition and sorting process, Reference [23] mentioned that the capacity of acoustic nuts separation could achieve about 40 pieces per second with a classification accuracy of around 97%.

Damaged nuts have significantly different characteristics on impact AE, since their inner structures are changed but compared with normal nut pieces, they still keep the same external forms and shapes. A similar situation was found in crushed ELV plastics scraps. In order to reduce the weight of vehicles and reduce the costs, most plastic parts of vehicles are molded to have a hollow structure, hence most of the scrap shapes are found to be homogenous after crushing: generally they are flexure or non-flexure flakes, other shapes are rare, less than 5% in mass [21,22]. Therefore in principle, impact AE recognition could also be used for the sorting of crushed ELV plastic materials—the mechanical and geometrical structures of crushed plastic scraps are much simpler than nuts. Correlative researches [27,28] have shown that, characteristics of impact AE signals depend only on the mechanical and geometrical properties of the specific materials, theoretically crushed plastic scraps could be also recognized by using impact AE characterization. However, so far, related research has not been carried out. The aim of this work was preliminary research on the feasibility of impact AE sorting of crushed plastic scraps as a further development and optimization of existing traditional and sensor based sorting processes. Three kinds of commonly utilized vehicle plastic materials were used for this research.

2. Methods and Materials

2.1. Design of Impact Tests

Vehicle plastic materials have similar mechanical properties to metallic materials which are substituted, such as high stiffness and impact resistance. Also, low velocity impacts between ASR plastic scraps and another rigid body are elastic collisions. This means before and after the impact process, kinetic energy loss is converted to vibration of both impacted bodies and then transferred to the ambient air as sound waves. Those sound waves carry characteristics of the impact materials as frequency responses.

It is generally understood that the impact AEs can be broadly divided into two parts: (a) sounds generated by the initially high surface acceleration and deceleration of impacting bodies found during the time of contact and (b) ringing sounds arising from the free-vibration of the bodies following the impact [29]. Ringing sounds which control the frequency response after the decay of the acceleration component have been traditionally recognized as useful for integrity inspection of material structures carried out in previous studies [27,28]. According to earlier research [27–30], for an impact between the flake structure scrap and a plate with larger mass and thickness than the tested scrap, as much as possible of the kinetic energy from a falling scrap should be converted to its own flexural-mode

free-vibration, *i.e.*, the ringing response or resonance which locates in the specific frequency domain. Hence all of the falling scrap pieces were designed to impact on a heavy stone plate which was sealed in an empty medium—density fiberboard (MDF) case whose inner surface is covered by sponge material in order to avoid the influence of ambient noises. The impact test chamber is shown in Figure 1.



Figure 1. Stone plate for impact test and impact acoustic emission (AE) acquisition chamber.

The stone plate was set near to the bottom of the chamber at an angle of 30° downward. Also, the height for scrap dropping was set at 750 mm.

2.2. Characterization of Impact AE Frequency Response

Theoretically impact AE frequency response signals can be written as follows:

For convenience, we consider the crushed plastic scraps approximately as circular flakes with different diameters, which are equivalently determined by their particle sizes through fine sieving. According to vibration principles, the equation of motion for flexural waves in a uniform thin plate along the transverse axis z is:

$$\frac{\partial^2 z}{\partial t^2} + \frac{Eh^2}{12\rho(1-\nu^2)} \nabla^4 z = 0 \tag{1}$$

where E is the material Young’s modulus, ρ is the material density, ν is the Poisson’s ratio of material, and h is the flake thickness.

For harmonic solutions, $z = Z(x, y)e^{j\omega t}$, where ω is the angular flexural vibration frequency:

$$\nabla^4 Z - \frac{12\rho(1-\nu^2)\omega^2}{Eh^2} Z = \nabla^4 Z - k^4 Z = 0 \tag{2}$$

where:

$$k^2 = \frac{\sqrt{12}\omega}{h} \sqrt{\frac{\rho(1-\nu^2)}{E}} = \frac{\sqrt{12}\omega}{c_p h} \tag{3}$$

c_p is the velocity of pressure wave in an infinite flake. In the case of a circular flake of radius b and thickness h , with fixed boundary, the frequency of flexural vibration is determined by equation [26]:

$$f_{m,n} = \alpha_{m,n} \sqrt{\frac{E}{\rho(1-\nu^2)}} \frac{h}{b^2} \tag{4}$$

where m and n are integers (beginning with zero), $\alpha_{m,n}$ is the coefficient associated with the corresponding flexural vibration mode (m, n), which depends on the impact position and shape of impact bodies. Equation (4) means that multiple-order flexural resonance could be generated by one flake, the frequency and amplitude of which depend on the impact position and the shape of physical void. In this research, all the falling scraps are of a flake structure and the experiment facility was designed to ensure that the impacts always occur on the surface edge of the falling scraps. Additionally, the second passive impact body is also fixed for all scrap impacts. Hence for the scraps of a specific material, the parameter $\alpha_{m,n}$ is a constant.

According to Equation (4), the material property parameters of ρ, E, b, h and are known, f can be obtained from impact AE signals. The Poisson’s ratio ν is a dimensionless quantity. It can be deduced that the unit of coefficient $\alpha_{m,n}$ should be mm/s or m/s, which are the units of velocity.

From Equation (4), the coefficient $\alpha_{m,n}$ could be further determined as a dimensionless quantity. Hence in this research, the impact frequency response for specific material depends only on the thickness and radius of single scraps. Combining the operation of all constants as k :

$$f = k \frac{h}{b^2}, \quad (k = \alpha_{m,n} \sqrt{\frac{E}{\rho(1-\nu^2)}}) \tag{5}$$

Obviously k is also a constant for the same material. The frequency response has been simplified to be a function of the particle size and thickness of single scrap particles and Equation (5) could be further normalized by standard thickness $h_{norm} = 1$ mm as: $\frac{f}{h} = k \frac{1}{b^2}$ and further:

$$f_{norm} = k h_{norm} \frac{1}{b^2} = k_c \frac{1}{b^2}, \quad (k h_{norm} = k_c, h_{norm} = 1 \text{ mm}) \tag{6}$$

The coefficient k_c has its units of mm²/s or m²/s. This coefficient indicates the variation of plastic materials.

Equation (6) describes the model of impact AE frequency response of flake scraps, it is nonlinear. The thickness of a single scrap could be determined precisely by using a laser triangulation method, which has already been widely applied for decades for volume stream measurement. The laser triangulation system is able to determine the height of a flake object within 20–100 ms.

Equation (6) also shows that for scraps from a specific kind of plastic, k_C is constant and their impact frequency response depends only on the thickness and particle size of a single scrap. The value of k_C varied according to the different plastic materials. Hence we could avoid direct measurement of the property parameters of specific materials, such as Young's modulus, density, Poisson's ratio *etc.* Different kinds of materials could be distinguished by determining the value of k_C by using fitting analysis of impact frequency responses.

2.3. Materials for This Research

Three kinds of plastics materials were sampled and implemented for this research, they are polypropylene (PP), acrylonitrile-butadiene-styrene (ABS) and styrene-maleic-anhydride (SMA). PP and ABS are commonly and widely used in most vehicles and SMA was commonly used in American automobile industries in the last decade and now commonly found in ELVs. All of the plastic materials were directly sampled from the corresponding parts of ELVs from an ELV authorized treatment facility, therefore the purity of each kind of material could be considered as 100%. Then similar to the ELV crushing process, the three kinds of material samples were crushed by a shredder with motor power of 37 kW under 1475 r/min, and a screen diameter of 23 mm. Ninety eight percent of PP, 95% of ABS and 96% of SMA scraps in the mass were found to have a flake structure.

For impact AE tests, the crushed scraps were further fine sieved according to sieving fractions within each millimeter from 3 mm to 23 mm. The scraps with particle sizes less than 3 mm could not be considered as having a flake structure. The scrap particle sizes were determined by the lower sieving fraction, e.g., the scraps of the sieving fraction $8 \text{ mm} < d < 9 \text{ mm}$ were considered to have an equivalent diameter of 8 mm.

3. Facility and Experimental Section

3.1. Experiment Facility

The thickness of a single scrap could be determined precisely by using laser triangulation, which has already been widely applied for decades for volume stream measurement. The laser triangulation system could be installed at a specific distance ahead of the scrap volume stream and was able to determine the height of a flake object within 45 ms.

The experimental facility was established as in Figure 2.

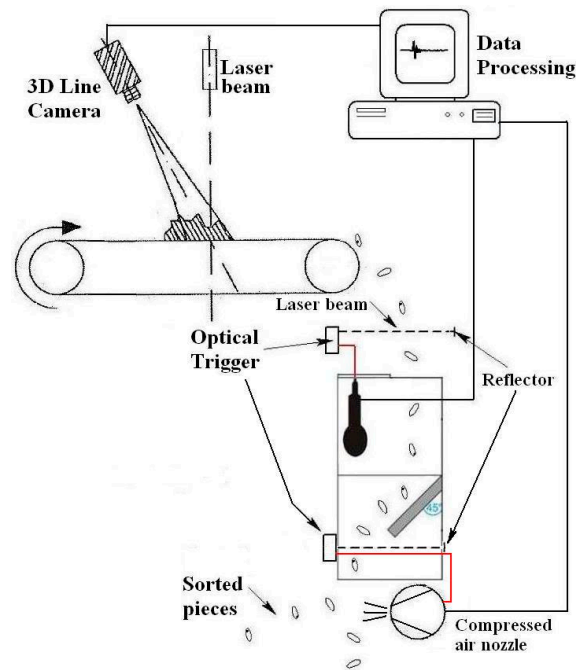


Figure 2. Experimental impact AE sorting facility.

The plastic scraps of specific particle size were individually fed onto a conveyor belt through a vibration feeder and then at the end of the belt they were dropped into the impact chamber in which the impact processes were implemented. Thicknesses of scraps were measured by laser beam and a camera installed above the conveyor belt and then the results stored in a computer. The AE pickup was installed inside the chamber. An optical trigger was fitted at the entrance of the chamber, by which the pickup could acquire the impact AE of the falling scraps sequentially according to the corresponding thickness data scraps. At the exit of the chamber there was also an optical trigger, which controlled a compressed air nozzle array together with a computer; the nozzle array had the same width as the exit of the chamber, which was able to blow every recognized scrap out of the main material stream and resulted in sorting tasks. The compressed air nozzle array is mainly used as an additional force field for different kinds of sensor aided sorting mechanisms. Reference [26] mentioned that the nozzle array separation frequency could achieve theoretically 40 pieces per second, but here in this research, in order to insure the sorting purity and efficiency, we tested the samples by using a feeding velocity of about 1–2 pieces/s. Under this velocity a sorting purity and efficiency of more than 99% could be achieved. Of course, sorting of flakes with extreme high purity and efficiency has already been implemented, for example, company TORMA has developed a facility with a sorting yield purity of up to 99% and an efficiency up to 97%, achieved under a feeding stream of 30 t/h.

All impact AE signals were acquired by an acoustic pickup, *i.e.*, an industrial microphone as analog signal input and then transferred to a soundcard where the analog signals were converted to digital signals. The A/D and D/A capacity of the soundcards are already adequate for industrial measurements and the prices of soundcards are much lower than professional devices. Normally a precision of 16 bit soundcards is better than the 12 bit professional data acquisition (DAQ) cards. Soundcards transfer data by Direct Memory Access (DMA) technology results in a massive reduction of the CPU occupation, which could realize high speed data communication. The Peripheral Component Interconnect (PCI) bus

technology allows high speed data communication between soundcard and system and makes online analysis and real time manipulation using virtual instruments possible.

3.2. Impact AE Signal Processing and Feature Extraction

Impact AE characterization was realized by AE signal processing and feature extraction.

Processing and analysis of impact AE signals were operated based on power spectrum density (PSD) method, it is a frequency spectral analysis based on the Fast Fourier Transformation (FFT) method. This method transfer AE signals from the time domain to the frequency domain, in which the frequency response distributions of impact are demonstrated as peaks.

The measurement threshold of the soundcard was 0–22 kHz, hence according to the Nyquist-Shannon sampling theorem the soundcard was set with a sampling rate of 44.1 kHz as well as a sampling number of 4096 for each AE signal data. Hanning window function was chosen for FFT operation in order to reduce side lobes and make the main feature peaks more significant. The original impact AE signal system contained white noise from electronic devices as well as AE signals from passive impact stone plate. Both kinds of noises could be eliminated by using an adaptive filter and band stop filter. For the facilities in this research, system electronic noise was determined to concentrate at around 500 Hz while the main lobe of stone plate impact AE responses focused on a range of 4350–4600 Hz. PSD spectra of a scrap impact AE signal before and after de-noising are shown in Figure 3.

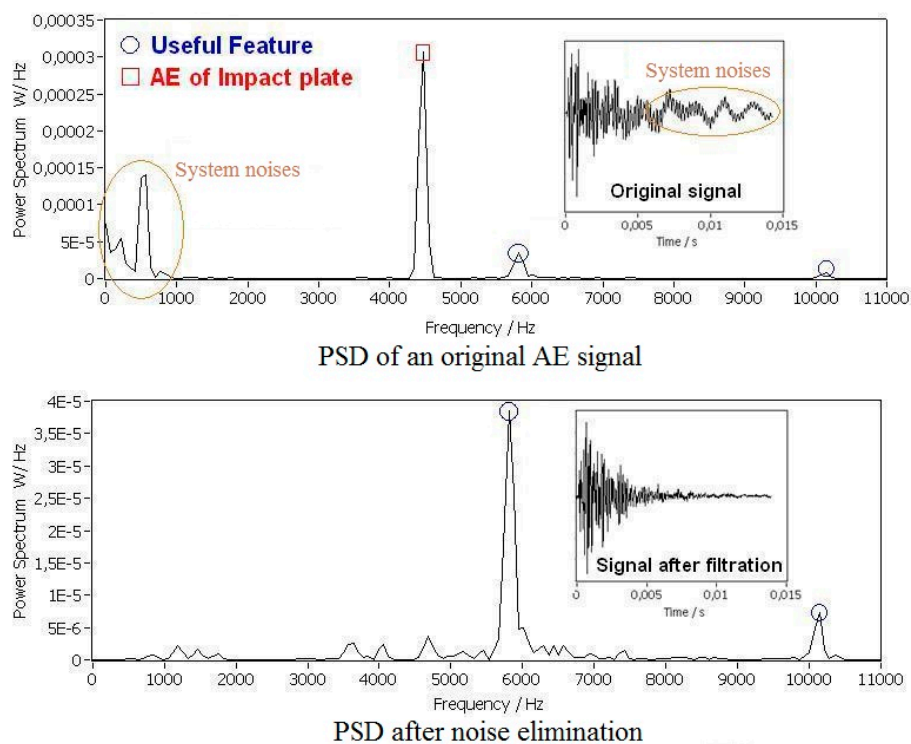


Figure 3. Power spectrum density (PSD) spectrum of an impact AE signal before and after filtration.

Figure 3 shows that the impact frequency response of this impact scrap concentrated on the position of the main peak/main lobe, around 5800 Hz. The lower peak around 10,000 Hz could be an

interharmonic of the impact AE signal, which is commonly generated by impulse signal and nonlinear frequency response models.

Feature extraction for impact AE recognition was realized by peak detection on the PSD spectral domain. With the help of programming in MATLAB, the coordinates of the main peaks and side peaks could be easily extracted. The main peaks indicated the concentration of frequency response energy, named as the eigen-frequency of a specific scrap. The feature extraction is shown in Figure 4.

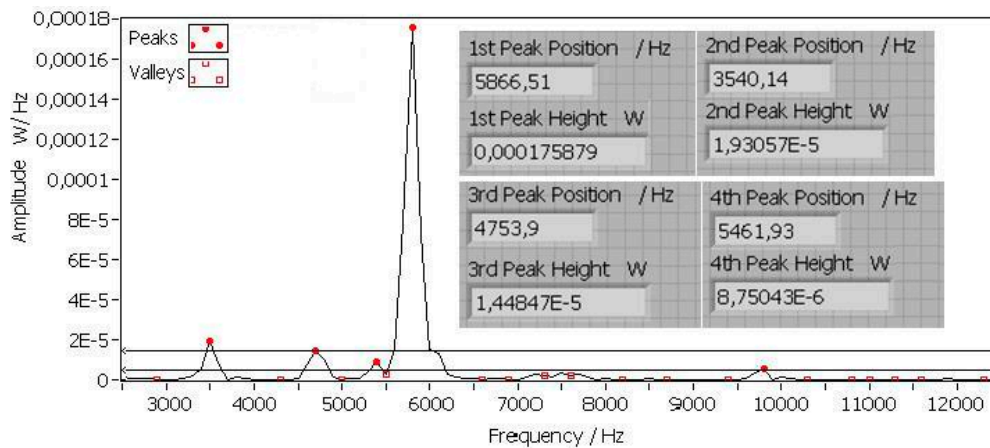


Figure 4. Feature extraction from PSD spectrum.

Generally, the main peak position in the PSD spectral domain indicated the impact response frequency of an impact scrap, described by Equation (5). Further by using the thickness of the scrap determined by laser-triangulation, the extracted eigen-frequency could be normalized to the eigen-frequency response f_{norm} . With f_{norm} from impact scraps of the same material, the material coefficient k_C could be obtained by data fitting and regression analysis according to the impact frequency response model of Equation (6).

4. Results and Discussion

4.1. Experiment Data

There were around three kinds of scrap samples, totally about 4.5 kg scrap was tested at about 1.5 kg per material. However, not all acquired AE signals were available for further processing and analysis. Several abnormal impacts generated irregular AE signals, which did not transfer enough energy for vibration but only for acceleration of rebound velocity. Big sizes of scrap pieces led occasionally to multi-impacts. Small mass scrap pieces could probably generate only weak signals which were covered in the background noise. Examples of weak signals and irregular signals are shown in Figure 5.

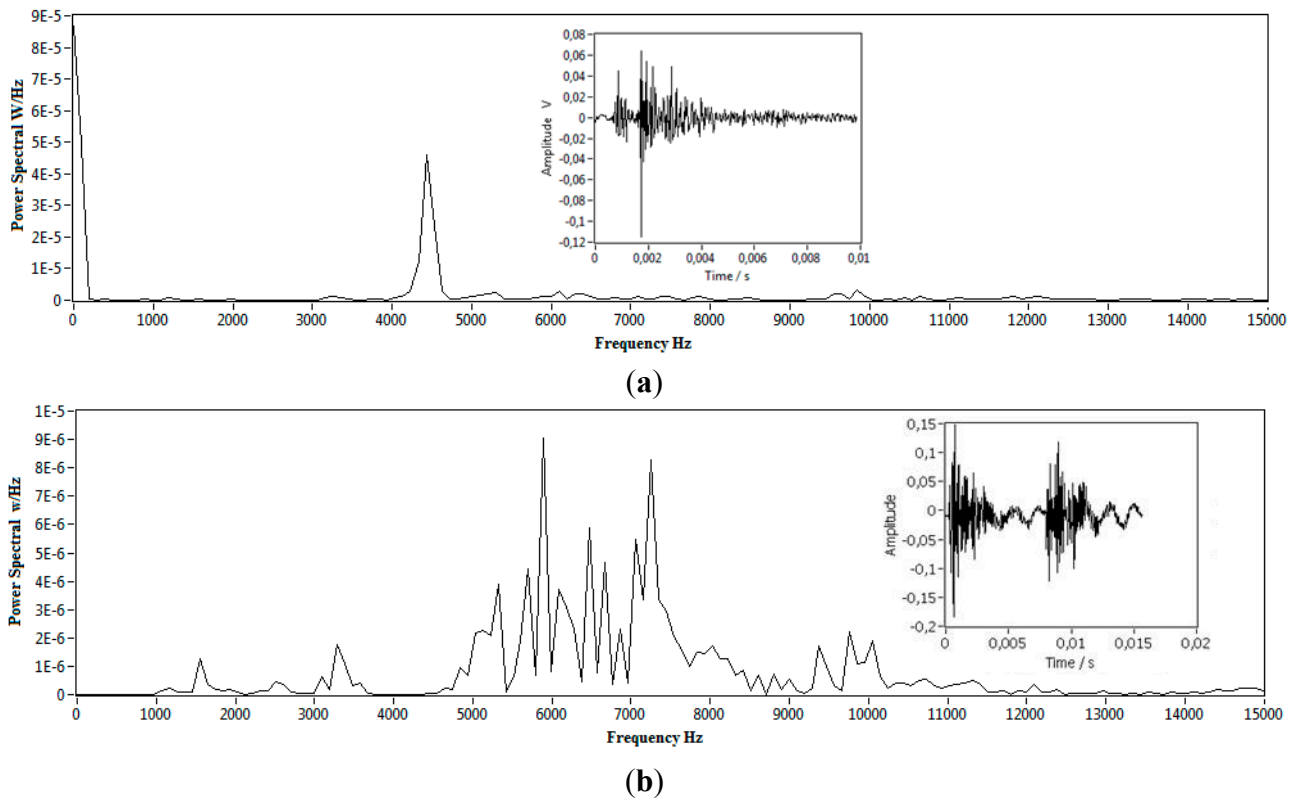


Figure 5. A weak signal and an irregular signal and their power spectrum, (a) low mass impact with only noise features; (b) low mass with double impact of one particle.

The AE signals from abnormal impacts and the signals of extreme low intensity were excluded. During the experiments, all of the scraps with diameters less than 8 mm resulted in inadequate intensity of the AE signals. Also, due to the crushing process, there were still several pieces of scrap with diameter larger than 23 mm remaining. The scraps with equivalent diameters of less than 8 mm and larger than 23 mm of PP, ABS, and SMA were 12.2%, 14.6%, and 13.8% in mass, respectively. Considering that 2% of PP, 5% of ABS, and 4% of SMA scraps in the mass were not flake structure, there were still 85.8% of PP scraps, 80.4% of ABS scraps, and 82.2% of SMA scraps remaining.

There were still quite a few weak signals found in the diameter range of 8–13 mm, which took more than 30% of all acquired signals. Considering this was a feasibility study, these weak signals were also excluded from further characterization. Although these signals were more intense than the signals with scrap diameters less than 8 mm, they were still not fully reliable because of the limitation of electronic devices, in which much useful signal information was hidden by noise.

The weak impact AE signals of scraps were clear enough for further characterization using more sensible electronic devices, such as AE pickup and sound acquisition hardware with higher S/N ratio and sensitivity. The proportions of PP, ABS, and SMA scraps with diameters from 8–13 mm were 16.8%, 16.6%, and 15.6% in mass respectively. With increasing scrap diameter, the intensity of the AE signals obviously also increased.

The scraps with abnormal impact of PP, ABS, and SMA were 4.4%, 2.1% and 2.7% in mass, respectively. Therefore the materials available for feature extraction remained 64.6% of PP, 61.7% of ABS, and 63.9% of SMA in mass, respectively. Overall there were about 1200 scrap impacts of each kind of material successful in feature extraction.

4.2. Eigen-Frequency Fitting and Regression Analysis

The fitting analysis of the acquired impact frequency responses started from a scrap diameter of 14–23 mm. The fitting model of impact eigen-frequency response is introduced by Equation (9). The resulting curves are shown as follows in Figure 6 for PP, ABS, and SMA scraps with different color, respectively.

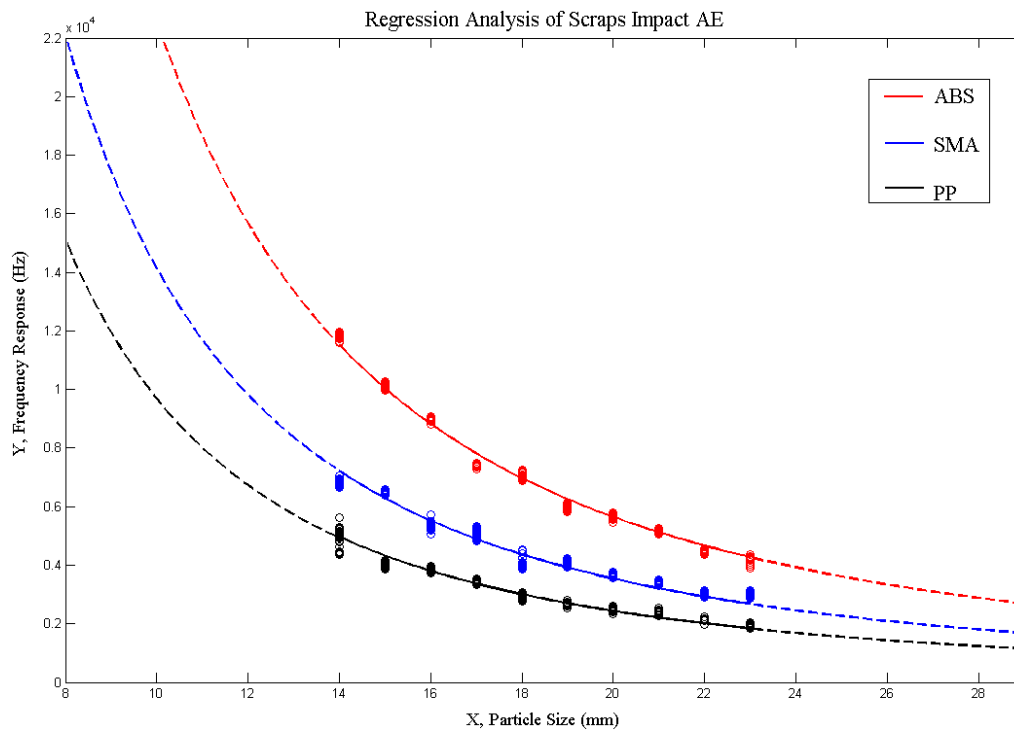


Figure 6. Fitting results of all three kinds of material.

The goodness of fit R^2 for PP, ABS, and SMA is 0.873, 0.911, and 0.866, respectively.

In Figure 6, the impact eigen-frequency responses of PP scraps were fitted to a unique curve with model parameter $k_c = 242.78 \text{ m}^2/\text{s}$. The impact eigen-frequency responses of ABS scraps were fitted to a unique curve with model parameter $k_c = 564.23 \text{ m}^2/\text{s}$. Additionally, the impact eigen-frequency responses of SMA scraps were fitted to a unique curve with model parameter $k_c = 353.33 \text{ m}^2/\text{s}$. In this figure, a solid line illustrates the curve fitted by experimental data, and the dotted line means the expectation of impact AE responses, extracted from other sizes of scraps which currently cannot be observed with actual devices. Here we expanded the diameter range to 8–29 mm.

The curves of impact eigen-frequency responses of ABS scraps shows that the f_{norm} of ABS scrap impacts were expected to extend across the upper hearing threshold of 22 kHz, when scrap diameters were less than 10 mm, whose impact AE signals could no longer be acquired by a traditional soundcard, and professional ultrasonic signal acquisition hardware was required. The PP scraps with diameter less than 6.64 mm and SMA scraps with diameters less than 8 mm are in the same situation.

Figure 6 also shows that the curves of impact eigen-frequency response were expected to get closer with increasing scrap diameters, and with decreasing scrap diameters, the curves moved further apart from each other. The vertical distance between the curves of corresponding materials depends on the variation of k_c , *i.e.*, the farther the vertical distance between adjacent curves, the higher the separation

rate of the corresponding plastic scraps could be obtained. Obviously here the PP scraps could be distinguished more accurately from ABS than SMA.

By fitting residue distribution analysis of the PP curve, we found that with a confidence level of 100% for PP, the fitting residues located within a range of ± 400 Hz. Also, the SMA scraps have a relative wider residue distribution, which covers the range of ± 600 Hz with a confidence level of 100%. ABS fitting residues are distributed in the range from -600 Hz to $+400$ Hz with confidence level of 100%. The 100% confidence intervals of the three materials did not have overlap, which meant that scraps of all three tested plastics could be completely distinguished.

For other plastic material mixtures with more similar values of k_c , their corresponding 100% confidence interval overlapped, which meant the scraps, whose impact eigen-frequency responses were located in the overlapped area could be miss-characterized and further influence the purity of the separation products. Therefore, with really closed curves, in order to avoid the confusion of overlapping we needed to narrow the confidence intervals, *i.e.*, reduce the characterization/separation rate to insure competent purity of the separation products. The curves that have an adequate distance between each other do not have such a problem and theoretically the corresponding scraps are expected to be sorted accurately and completely.

Finally through this experiment, 64.6% of PP scraps, 61.7% of PP scraps, and 63.9% of SMA scraps in mass were successfully characterized and further sorted.

5. Conclusions

According to the results of this research, the following conclusions were obtained:

- (1) With the actual experimental facilities and electronic devices, 64.6% of PP scraps, 61.7% of ABS scraps, and 63.9% of SMA scraps in mass respectively were successfully characterized, with diameters from 14–23 mm. The feeding velocity of the tested scraps was 1–2 pieces/s.
- (2) The larger the variation of the material coefficient k_c , the higher the efficiency of characterization/separation, and *vice versa*. The value of k_c depends only on material mechanical properties.
- (3) Fitting curves demonstrated that scraps with lower diameters were expected to be more easily recognized and separated than scraps with larger diameters. However, the impact eigen-frequency response of smaller scrap was located beyond the hearing threshold. In this case, a professional AE signal acquisition device was necessary.
- (4) Characterization and separation by using impact AE completely avoided the influence of black, dark or color dyes, as well as the supporting additives in vehicle plastics, which caused great difficulty in other sorting methods.
- (5) Different automobile enterprises have their own formulas for dyeing, modification, and reinforcement on vehicle plastics. By way of commercial confidentiality, the compositions of plastic materials are difficult to obtain from manufacturers, even with the aim of recycling. The method of using impact AE recognition could avoid this problem, since it concentrates only on the mechanical properties of vehicle plastics, which are normally open in design.

- (6) With the actual experiment facilities and devices, not all impact AE signals were available for analysis. More convenient facilities and sensitive signal acquisition devices are necessary. The crushing process and facilities also need to be modified, in order to increase the scrap proportions with the appropriate particle size.
- (7) This research concentrated on sorting of plastic scraps with flake or quasi-flake structures. Although this shape of plastic scraps makes up the vast majority, the development of an impact frequency response model for other scrap shapes is also necessary in subsequent research.

Generally, this research verified the feasibility of sorting ASR plastic materials by using impact acoustic emission processing and characterization. This method can be an appropriate solution for optimization of existing ELV plastics' recycling technologies. Further in-depth research in signal processing and the elastic collision model are required. Additionally, this feasibility study should be further extended to other kinds of vehicle plastics.

Acknowledgments

This research was financially supported by projects “China Fundamental Research Funds for the Central Universities 2015QNA28” and “The Funds for Creative Research Groups of China 51421003”, The contribution of Thomas Pretz and colleagues in department of processing and recycling, RWTH Aachen University in Germany were highly appreciated by the authors.

Author Contributions

The author Jiu Huang contributed research and experimental work in this study. And the authors Zhengfu Bian and Shaogang Lei contributed data analysis work and revision of this paper.

Conflicts of Interest

The authors declare no conflict of interest.

Glossary

E	Young's modulus (N/m ²)
ρ	material density (kg/m ³)
ν	Poisson's ratio of material
h	scrap thickness (m)
b	equivalent radius of scraps (m)
f	impact frequency response (Hz)
$\alpha_{m,n}$	vibration mode coefficient (m/s)

References

1. Granata, G.; Moscardini, E.; Furlani, G.; Pagnanelli, F.; Toro, L. Automobile shredded residue valorisation by hydrometallurgical metal recovery. *J. Hazard. Mater.* **2011**, *185*, 44–48.

2. Gent, M.R.; Menéndez, M.; Muñiz, H.; Torno, S. Recycling of a fine, heavy fluff automobile shredder residue by density and differential fragmentation. *Waste Manag.* **2015**, *43*, 421–433.
3. Vermeulen, I.; van Caneghema, J.; Blocka, C.; Baeyens, J.; Vandecasteele, C. Automotive shredder residue (ASR): Reviewing of its production from end-of-life vehicles (ELV's) and its recycling energy or chemical's valorization. *J. Hazard. Mater.* **2011**, *190*, 8–27.
4. Nakanishi, H.; Black, J. Social Sustainability Issues and Older Adults' Dependence on Automobiles in Low-Density Environments. *Sustainability* **2015**, *7*, 7289–7309.
5. Dai, J.Q.; Huang, H.F. *Introduction to Circular Economy*; Science Publishing Inc.: Beijing, China, 2009; pp. 202–204.
6. Zhou, Z.Q.; Dai, G.H.; Tan, H.M. Review of Dismantling and Recycling Technology for End-of-Life Vehicle. *J. Changshu Inst. Technol.* **2011**, *25*, 107–111.
7. Guo, Q.J.; Zhang, X.; Li, C.; Liu, X.M.; Li, J.H. TG-MS study of the thermo-oxidative behavior of plastic automobile shredder residues. *J. Hazard. Mater.* **2012**, *209–210*, 443–448.
8. Singh, J.; Lee, B.K. Reduction of environmental availability and ecological risk of heavy metals in automobile shredder residues. *Ecol. Eng.* **2015**, *81*, 76–81.
9. Lee, C.H.; Truc, N.T.T.; Lee, B.K.; Mitoma, Y.; Mallampati, S.R. Evaluation of heavy metals in hazardous automobile shredder residue thermal residue and immobilization with novel nano-size calcium dispersed reagent. *J. Hazard. Mater.* **2015**, *296*, 239–247.
10. Mancini, G.; Viotti, P.; Luciano, A.; Fino, D. On the ASR and ASR thermal residues characterization of full scale treatment. *Waste Manag.* **2014**, *34*, 448–457.
11. Mancini, G.; Viotti, P.; Luciano, A.; Raboni, M.; Fino, D. Full scale treatment of ASR wastes in a modified rotary kiln. *Waste Manag.* **2014**, *34*, 2347–2354.
12. Mancini, G.; Tamma, R.; Viotti, P. Thermal process of fluff: Preliminary tests on a full-scale treatment plant. *Waste Manag.* **2010**, *30*, 1670–1682.
13. Morselli, L.; Santini, A.; Passarini, F.; Vassura, I. Automobile shredder residue (ASR) characterization for a valuable management. *Waste Manag.* **2010**, *30*, 2228–2234.
14. Santini, A.; Passarini, F.; Vassura, I.; Serrano, D.; Dufour, J.; Morselli, L. Auto shredder residue recycling: Mechanical separation and pyrolysis. *Waste Manag.* **2012**, *32*, 852–858.
15. Passarini, F.; Ciacci, L.; Santini, A.; Vassura, I.; Morselli, L. Auto shredder residue LCA: Implications of ASR composition evolution. *J. Clean. Prod.* **2012**, *23*, 28–36.
16. Nourreddine, M. Recycling of auto shredder residue. *J. Hazard. Mater.* **2007**, *139*, 481–490.
17. Liu, F.; Xu, D.M. Recycling and Utilization of PP bumpers (In Chinese). *China Resour. Compr. Util.* **2007**, *9*, 11–13.
18. Gent, R.; Menéndez, M.; Toraño, J.; Diego, I. Recycling of plastic waste by density separation: Prospects for optimization. *Waste Manag. Res.* **2009**, *27*, 175–187.
19. Ferrão, P.; Nazareth, P.; Amaral, J. Strategies for meeting EU end-of-life vehicle reuse/recovery targets. *J. Ind. Ecol.* **2006**, *10*, 77–93.
20. Pretz, T.; Wotruba, H.; Nienhaus, K. *Application of Sensor-Based Sorting in Raw Material Industry*; Shaker Publishing House Co. Ltd.: Aachen, Germany, 2011; pp. 139–141.
21. Huang, J.; Pretz, T.; Bian, Z.F. Automatic sorting of solid black polymer wastes based on visual and acoustic sensors. In Proceedings of the 3rd International Conference on Environmental and Computer Science, Kunming, China, 10–12 September 2010.

22. Huang, J.; Pretz, T.; Bian, Z.F. Intelligent solid waste processing using optical sensor based sorting technology. In Proceedings of the 3rd International Congress on Image and Signal Processing, Yantai, China, 16–18 October 2010.
23. Huang, J.; Pretz, T. Akustische sortierung für dunkle Kunststoffe. *Recycl. Technol.* **2010**, *9*, 38–40.
24. Giaime, G.; Guisto, D.; Märgner, V.; Meinlschmidt, P. Detection of foreign bodies in food by thermal image processing. *IEEE Trans. Ind. Electron.* **2004**, *51*, 480–490.
25. Renzi, M.; Balducci, B. Development of Italian particle board production in a European context. In Proceedings of the 5th European Wood Based Panel Symposium, Hanover, Germany, 4–6 October 2006.
26. Person, T.; Cetin, A.; Tewfik, A.; Haff, R. Feasibility of impact acoustic emission for detection of damaged wheat kernels. *Digit. Signal Process.* **2007**, *17*, 617–633.
27. Tong, F.; Tso, S.K.; Huang, M.Y. Tile-Wall bonding integrity inspection based on time-domain features of impact acoustics. *Sens. Actuators A Phys.* **2006**, *132*, 557–566.
28. Tong, F.; Xu, X.M.; Luk, B.L.; Liu, K.P. Evaluation of Tile-Wall bonding integrity based on impact acoustics and support vector machine. *Sens. Actuators A Phys.* **2008**, *134*, 97–104.
29. Christoforou, A.; Yigit, A. Effect of flexibility on low velocity impact response. *J. Sound Vib.* **1998**, *217*, 563–578.
30. Rossing, T.; Flechter, N. *Principles of Vibration and Sound*; Springer-Verlag: New York, NY, USA, 1994; pp. 311–316.

© 2015 by the authors; licensee MDPI, Basel, Switzerland. This article is an open access article distributed under the terms and conditions of the Creative Commons Attribution license (<http://creativecommons.org/licenses/by/4.0/>).